Airfoils in Cross Flow

Thomas Staubli
LUASA, Lucerne, Switzerland

Roger Waser
LUASA, Lucerne, Switzerland

Christian Widmer
LUASA, Lucerne, Switzerland

ABSTRACT

The investigated airfoil in cross flow is excited to transverse oscillations of large amplitudes in a broad band of flow conditions.

The study involves experiments in a water channel and numerical flow simulations both with forced and free oscillations.

Experiments and simulations confirm the same basic excitation mechanisms, which are on the one hand vortex induced oscillations and on the other hand movement induced excitations.

For flow conditions where the frequency of the natural vortex shedding is well below the natural frequency of the airfoil in transverse direction hard excitation is needed to initiate oscillations. When the frequency of the vortex shedding is close to or slightly below the natural frequency of the airfoil self-excited vortex induced oscillations start and movement induced excitation leads to very high oscillation amplitudes. For vortex shedding frequencies higher than the natural frequency of the mechanical system no oscillations are excited.

1. INTRODUCTION

Airfoils are designed to provide good lift to drag ratios. However, when exposed to cross flow, flow separations will occur on both, the leading and the trailing edges. As well known from bluff body aerodynamics alternate vortex shedding will arise. If airfoils are exposed to cross flow and if they are free to move in transverse direction, then high amplitude self-excited oscillations may build up at frequencies at and above the natural vortex shedding frequency.

The phenomenon of such excitation is comparable to the excitation of D-shaped sections as described by Feng (1969), Novak (1974), or Bardowicks (1976), however, much higher amplitudes are observed for airfoils due to the lower resistance in transverse direction compared to the D-section.

Using the classification introduced by Naudascher and Rockwell (1974) we find alternate vortex shedding (AVES) for the non-oscillation airfoil. Once oscillations start, impinging leading edge vortices (ILEV) are observed which attach to the back side of the profile during almost half a cycle of the oscillation. During the return cycle the former trailing edge becomes now leading edge and a vortex of opposite rotation is attaching to the profile.

For natural frequencies of the airfoil (in transverse direction) close to the natural vortex shedding frequency oscillation will be self-excited. This is typical for so-called instability induced excitation, IIE.

For natural frequencies of the airfoil higher than the natural vortex shedding frequency this oscillation will not be self-excited, an external disturbance is needed to start the oscillations. Once started the amplitudes may become very large. This effect is typical for so-called hard oscillations. Since an initial transverse motion of the profile is condition for the excitation, the classification is movement induced excitation, MIE.

Galloping oscillations belong to this class of MIE. Galloping oscillations, fulfilling the Den Hartog criterion, e.g. Novak 1972, typically are observed at low frequencies, well below the natural vortex shedding frequency, or speaking in terms of reduced velocities, at reduced velocities well above that where the natural vortex shedding occurs. In contrast, the oscillations discussed in this paper refer to oscillations at or above the natural vortex shedding frequencies. Galloping oscillations and the oscillations reported here have the very high amplitudes in common and belong both to the class of MIE.

Best known and most feared is this MIE type of excitation with sailing boats. If sails are exposed to cross flow the boats eventually start to roll fiercely. The so called death roll often results capsizing of dinghy boats or for keel boats in destruction of the spinnaker pole or even in demasting the boat. This phenomenon is best described by Marchaj (1985).

2. DEFINITIONS

Figure 1 explains the motion, the used co-ordinate system and the absolute and relative flow direction. If there is a force component, $c_y(t)$, acting in phase with the velocity $\dot{y}(t)$ of the profile then an energy transfer from the fluid to the body will arise and excitation may occur if the energy dissipated in the mechanical system is smaller than the energy input.

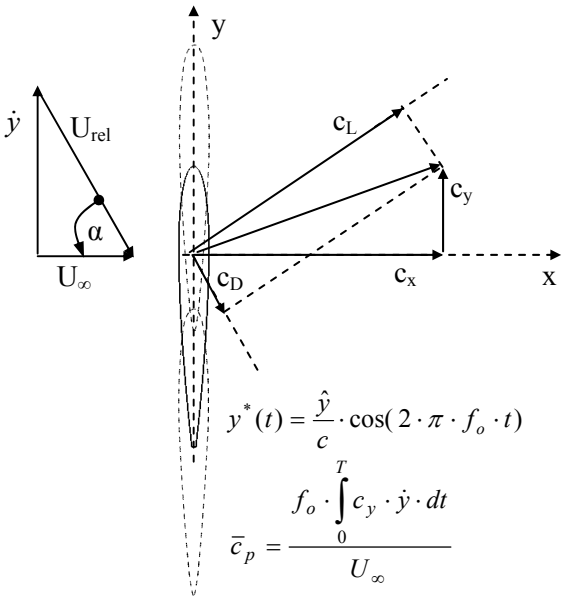

Figure 1: *Airfoil in cross flow.*

The product of chord c and the airfoil length l defines the area A with which force coefficients are determined.

Further definitions:

U_∞ = undisturbed flow velocity
c = chord length
S = Strouhal number
y^* = y/c = nondimensional displacement
$\hat{y}^*$ = $\hat{y}$/c = nondimensional amplitude
f_o = oscillation frequency
f_n = natural frequency of the mechanical system in transverse direction
f_n^* = f_n/f_n = 1 = standardized natural frequency
f_{no} = natural vortex shedding frequency of the non oscillating profile = $U_\infty S/c$
U^* = reduced velocity = $f_{no}/f_o = 1/f_o^*$
f_o^* = f_o/f_{no} = nondimensional oscillation frequency
f_v = vortex shedding frequency of oscillating profile
f_v^* = f_v/f_n = nondimensional vortex shedding frequency of the oscillating profile
c_p = power coefficient

3. EXPERIMENTS

Experiments were carried out with a NACA0011 profile of chord 31.5mm in a perspex water channel with a flow cross section of 1m width and a water depth of 0.22 m. Velocities were varied between 0.2 and 0.4 m/s.

Flow visualization was performed using the hydrogen bubble technique. Displacement was measured using a Laser optical device.

On the one hand the free oscillations were investigated. The profile was suspended from a low friction mechanical device allowing transverse oscillation. Parameters varied in the experiments were the spring and the damping of the mechanical oscillator system. Details of the experimental equipment are described by Widmer (2007).

Due to the low stiffness of the airfoil in flow direction a minor secondary motion at twice the oscillation frequency was observed in x-direction. In spite that these amplitudes were small they had an important impact on the transverse oscillation. With an increase of such inline oscillation also an increased damping effect of the transverse oscillations was observed.

On the other hand also forced oscillation experiments by driving a harmonic motion in transverse direction of varying amplitude and frequency were carried out, Eichholzer (2007).

Figure 2 displays a typical case of vortex shedding observed for oscillations at 2.7 times the frequency of the natural vortex shedding frequency.

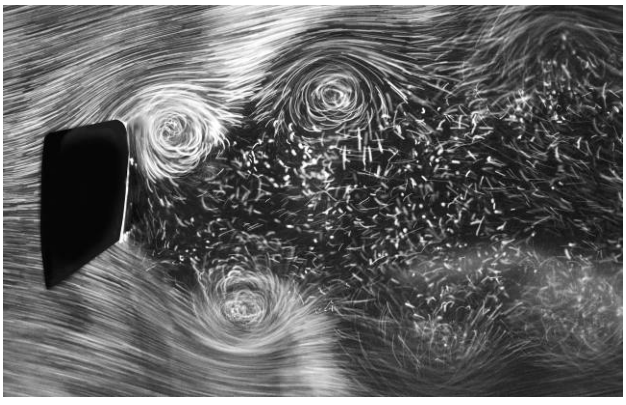

Figure 2: *Vortex shedding in the wake of the airfoil at f_o^*=2.7 and $\hat{y}^*$ = 0.33.*

Figure 3 shows the influence of a varying excitation frequency on the vortex formation frequency f_v for a selected constant amplitude. The dotted line indicates the line with $f_v = f_{no}$. The shedding frequency starts to synchronize with the oscillation frequency at about 0.8 times the natural vortex shedding frequency. For higher oscillation frequencies the vortex shedding remains locked to the oscillation frequency in the entire investigated frequency range. It is this range above $f_o^* = 1$ where

the freely suspended profile is excited to oscillate. Above $f_o^* = 2$ only hard excitation leads to oscillations.

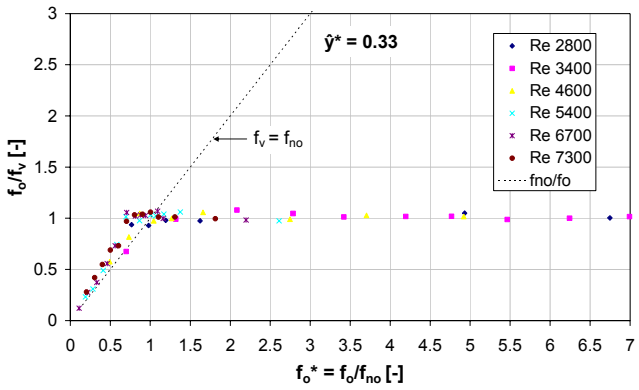

Figure 3: *Vortex shedding frequencies for forced oscillations for different Reynolds numbers.*

The experiments have been performed at various flow velocities, but there is no indication that the Reynolds number has a major influence on synchronization mechanisms. However, the investigated Reynolds numbers are well below numbers typically encountered in technical problems. In order to overcome this drawback additional numerical simulations were performed at very high Reynolds numbers.

4. NUMERICAL FLOW SIMULATION

The computations were performed with ANSYS CFX 11.0, a commercial finite volume CFD code. The turbulence model used for all the computations is the SST (shear stress transport) model. All the computations were performed in unsteady mode (URANS), with a second order discretization scheme in space and time.

The mesh was generated with ICEM CFD version 11.0. A structured mesh of 10^5 elements showed to be adequate. The mesh quality check showed that:

- The smallest angle was larger than 34 degrees.
- The maximum aspect ratio of the elements is below 18 in the boundary layer and below 44 in the outer flow.
- The average y+-values were 8.3 (maximum 11)
- The maximum volume change of the elements was below 1.6.

All simulations were done in 2-D in spite that in reality there will be spanwise deformations of the vortices to a certain amount. Furthermore, the SST-model uses in the outer flow the kε-model, which in turn is not well suited for prediction of vortical structures. Since in this particular case dynamic flow separation, reattachment and large amplitude oscillations are dominant, it can be assumed that the simulations will give at least qualitatively correct results. Simulations with the non-oscillating profile resulted in the correct prediction of the Strouhal number.

For simulation of the profile oscillations the moving mesh method was applied. In order to avoid negative influence on the mesh quality a region around the profile was defined where no mesh deformation was allowed. In this region with a diameter of 3 chord length mesh elements were only displaced, but not deformed. The mesh deformation was realized in the outer zone by deforming the elements linearly up to the boundaries of the computational domain.

Different types of simulations were performed. On the one hand fluid forces were determined in the case of forced oscillation with prescribed motion and on the other hand free oscillations were simulated by coupling the simulated flow domain with the differential equations of a simple one mass oscillator.

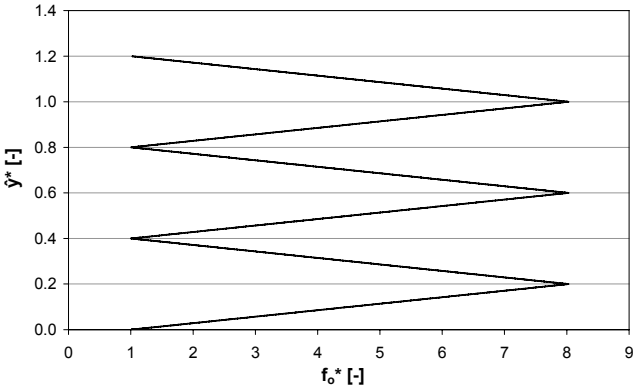

Figure 4: *Forced oscillations with varying frequencies and amplitudes.*

For the case of forced oscillation with prescribed motion a new method was developed to get most information out of one single transient simulation. Like this the computational effort could be considerably reduced. During the transient simulations the forcing frequency was alternatively linearly increased and decreased while the displacement amplitude was constantly increased (Figure 4). Force coefficients were fitted for each oscillation cycle and the power was determined by multiplying force and displacement velocity. Positive power coefficients stand for an energy transfer from the flow to mechanical system and thus for possible excitation.

5. RESULTS

5.1 Forced oscillations

As shown in Figure 5 simulation of forced oscillations revealed positive values of the power coefficient in a broad band above the frequency ratio $f_o^* =$

$f_o/f_{no} = 1$ where the oscillation frequency is identical with the natural vortex shedding frequency f_{no} of the non-oscillating profile.

According to the simulations a positive energy transfer is observed for amplitudes of up to 1.5 chord lengths. The maximum energy transfer is observed for excitation frequencies between 2 and 3 times f_{no}. In this range the largest power coefficients were calculated. This finding was confirmed by the experiments. The visualization of Figure 2 lies in this range of maximum excitation.

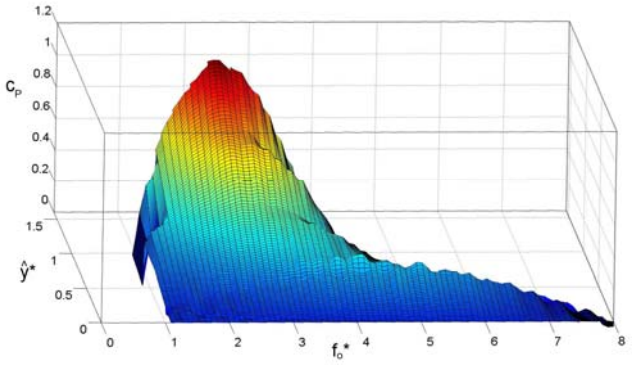

Figure 5: *Power coefficient for forced oscillations.*

In the entire range of positive power coefficients displayed in Figure 5 vortex shedding in the wake is synchronized with the oscillation frequency f_o, an other finding confirmed by the experiment, as can bee seen in Figure 3.

Also the simulations have been performed at different Reynolds numbers and, as in the experiment, no major influence on synchronization mechanisms was found.

In addition to the water simulations, further simulations were carried out with air, a profile of chord length 2.3m, and a wind speed of 15m/s. Again very similar synchronization behavior was found at these by orders of magnitude higher Reynolds numbers.

5.2 Free oscillations

Free oscillations of the airfoil in cross flow were simulated by coupling the fluid forces with the differential equations of simple one mass oscillators.

$$m \cdot \ddot{y} + d_{mech} \cdot \dot{y} + c_{Spring} \cdot y = F_{y\,Fluid}$$

For each time step the displacement is adjusted such that the mechanical forces and the fluid forces are in equilibrium. Mechanical stiffness, damping, and mass were adjusted to fit the experiment.

For integration a Runge Kutta procedure of forth order was applied. For each new time step displacement, velocity, and acceleration is taken from the previously simulated point.

Figure 6 displays a simulated case were the flow velocity was gradually increased during a time interval corresponding to about 90 periods of the mechanical system, $T = 1/f_o$. The displayed reduced velocity U^* actually can be interpreted as the frequency ratio of the vortex shedding frequency of the non-oscillating airfoil f_{no} and the oscillation frequency f_o since $U^* = U_\infty S/f_o c = f_{no}/f_o$, with S = 0.14 = Strouhal number of the profile.

At a reduced velocity of $U^* \approx 0.9$ self excited oscillation started and the vortex shedding frequency f_v synchronized with f_o. It has to be noted that once the airfoil started to oscillate in transverse direction, it oscillated at the natural frequency f_n of the mechanical system.

In the range between 90 and 180 periods the velocity was kept constant until stationary oscillations were observed.

From 180 to 220 periods the velocity was reduced to its initial value. During the down slope displacement amplitudes increased further to decay then asymptotically to a constant value. The vortex shedding remains synchronized. Thus, for the same flow condition no oscillation occur at the beginning and high amplitudes at the end. This indicates a hysteresis effect and supports the experimental finding that for $U^* = f_{no}/f_o < 0.5$ ($f_o^* > 2$) hard excitation is necessary condition for oscillations.

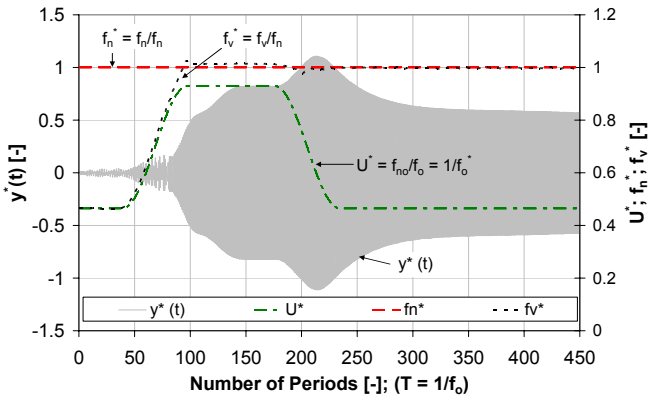

Figure 6: *Simulated hysteresis of free oscillator.*

The comparable experiments are displayed in Figure 7. The flow velocity was increased gradually until self-excited oscillations did build up. The increase of the velocity was stopped at $U^* = 0.92$. In contrast to the simulations it took more time for the self-excited oscillations to build up. When the flow velocity was reduced the amplitudes further increased, as in the comparable numerical simulation displayed in Figure 6. When the velocity reached the initial velocity again, stationary oscillations with amplitudes of 0.55 chord length were observed.

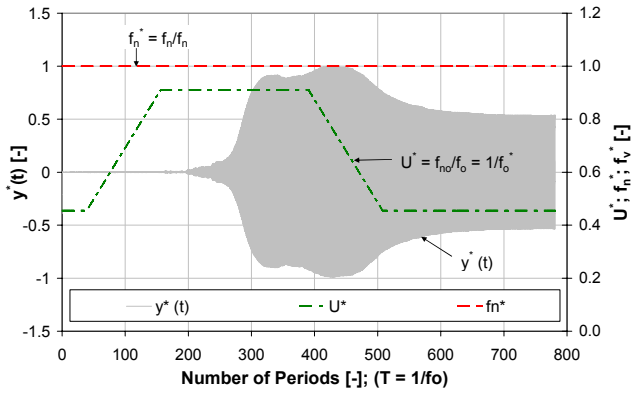

Figure 7: *Measured hysteresis of free oscillator.*

In a further experiment the flow velocity was increased well above synchronisation. Amplitudes immediately started to decay for reduced velocities $U^* > 1$. Figure 8 shows the entire range of self-excited oscillations for the given mechanical system.

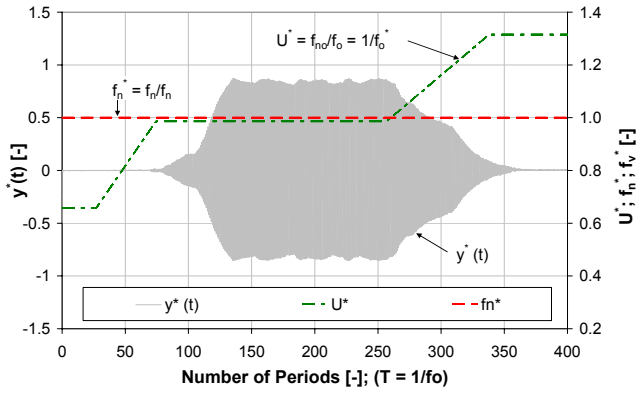

Figure 8: *Range of self-excited oscillations*

6. CONCLUSION

Airfoils in cross flow can be excited to very high amplitudes of oscillations in transverse direction due to MIE. Self-excited oscillations arise only when the flow velocity is such that the natural vortex shedding frequency is below and close to the natural frequency of the mechanical system in transverse direction ($2 > f_o^* = f_o/f_{no} > 1$ or $0.5 < U^* < 1$). For lower velocities hard excitation is possible. In this range movement induced oscillations may built up from an initial disturbance, e.g. a gust or a mechanical impact.

The power transferred to the airfoil increases with the 3rd power of the flow velocity. For this reason the highest risk for destructive oscillation is when the mechanical system has a natural frequency in transverse direction which is excited at high flow velocities.

To avoid such cases the natural frequency for systems with low damping should either be excited only at low flow velocities or the possible excitation range should be well above the highest flow velocity ($U^* < 1/8$).

Figure 9 gives an overview on the risk potential and the possible types of excitation of an airfoil in crossflow in the range of reduced velocities $1/8 < U^* < 1$.

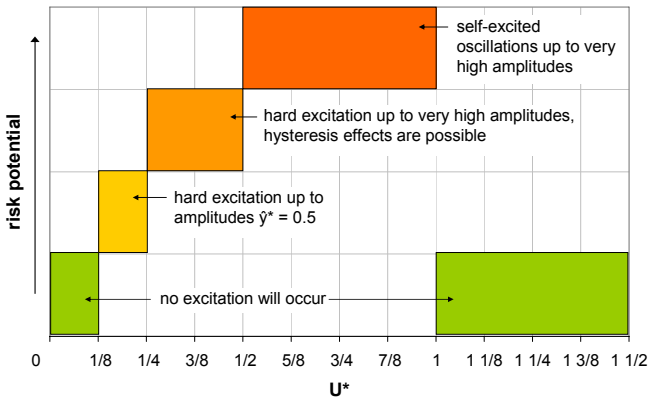

Figure 9: *Range of possible self-excited oscillations and hard excitation.*

General conclusion is that both, numerical simulations and experiments, led qualitatively to the same findings and allowed better understanding of the phenomena involved.

7. REFERENCES

Novak M., 1972, Galloping oscillations of prismatic structures. ASCE *Journal of the Engineering Mechanics Division* **98**: 27-41.

Novak M., Tanaka H., 1974, Effect of the turbulence on the galloping instability, *ASCE Journal of the Engineering Mechanics Division* **100**: 27–47.

Bardowicks H., 1976, *Untersuchung der Einflüsse von Querschnittsform und Schwingweite auf aeroelastische Schwingungen scharfkantiger prismatischer Körper*, Dissertation, Hannover

Naudascher E., Rockwell D., 1994, *Flow-Induced Vibrations - An Engineering Guide*, Rotterdam:. Balkema

Marchaj C.A., 1985, *Sailing Theory and Practice*, Dodd Mead

Widmer C., 2007, *Wirbelinduzierte Schwingungen eines querangeströmten Flügelprofils*, Diploma thesis, LUASA

Eichholzer S., 2007, *Untersuchung des fluiddynamischen Anregemechanismus an einem quer angeströmten schwingenden Flügelprofil*, student project, LUASA